

Article

# Highly Efficient DSSCs Sensitized Using NIR Responsive Bacteriopheophytine-a and Its Derivatives Extracted from Rhodobacter Sphaeroides Photobacteria

Abdulrahman I. Almansour, Raju Suresh Kumar <sup>\*</sup>, Khloud Ibrahim Al-Shemaimari and Natarajan Arumugam <sup>\*</sup>

Department of Chemistry, College of Science, King Saud University, P.O. Box 2455, Riyadh 11451, Saudi Arabia; almansour@ksu.edu.sa (A.I.A.); 442203282@student.ksu.edu.sa (K.I.A.-S.)

<sup>\*</sup> Correspondence: sraju@ksu.edu.sa (R.S.K.); anatarajan@ksu.edu.sa (N.A.)

**Abstract:** Employing naturally extracted dyes and their derivatives as photosensitizers towards the construction of dye-sensitized solar cells (DSSCs) has been recently emerging for establishing sustainable energy conversion devices. In this present work, Rhodobacter Sphaeroides Photobacteria (Rh. Sphaeroides) was used as a natural source from which Bacteriopheophytine-a (Bhcl) dye was extracted. Further, two cationic derivatives of Bhcl, viz., Guanidino-bacteriopheophorbide-a (Gua-Bhcl) and (2-aminoethyl)triphenylphosphono-bacteriopheophorbide-a (2AETPPh-Bhcl) were synthesized. The thus obtained Bhcl, Gua-Bhcl and 2AETPPh-Bhcl were characterized using liquid chromatography–mass spectrometry (LC–MS) and their photophysical properties were investigated using excitation and emission studies. All three near-infrared (NIR) responsive dyes were employed as natural sensitizers towards the construction of DSSC devices, using platinum as a photocathode, dye-sensitized P25-TiO<sub>2</sub> as a photoanode and I<sup>−</sup>/I<sub>3</sub><sup>−</sup> as an electrolyte. DSSCs fabricated using all three dyes have shown reasonably good photovoltaic performance, among which 2AETPPh-Bhcl dye has shown a relatively higher power conversion efficiency ( $\eta$ ) of 0.38% with a short circuit photocurrent density ( $J_{SC}$ ) of 1.03 mA cm<sup>−2</sup>. This could be attributed to the dye's natural optimal light absorption in the visible and NIR region and uniform dispersion through the electrostatic interaction of the cationic derivatives on the TiO<sub>2</sub> photoanode. Furthermore, the atomic force microscopy studies and electrochemical investigations using cyclic voltammetry, electrochemical impedance spectroscopy and Bode's plot also supported the enhancement in performance attained with 2AETPPh-Bhcl dye.

**Keywords:** DSSC; natural dye; Rhodobacter Sphaeroides; photosensitizer; TiO<sub>2</sub>

**Citation:** Almansour, A.I.; Kumar, R.S.; Al-Shemaimari, K.I.; Arumugam, N. Highly Efficient DSSCs Sensitized Using NIR Responsive Bacteriopheophytine-a and Its Derivatives Extracted from Rhodobacter Sphaeroides Photobacteria. *Molecules* **2024**, *29*, 931. <https://doi.org/10.3390/molecules29050931>

Academic Editors: Aleksandra Drygała and Janusz Wyrwał

Received: 30 December 2023

Revised: 16 February 2024

Accepted: 18 February 2024

Published: 21 February 2024



**Copyright:** © 2024 by the authors. Licensee MDPI, Basel, Switzerland. This article is an open access article distributed under the terms and conditions of the Creative Commons Attribution (CC BY) license (<https://creativecommons.org/licenses/by/4.0/>).

## 1. Introduction

In recent years, low production costs and ecologically favorable operation have made dye-sensitized solar cells (DSSCs) an immensely attractive energy conversion device. The working of DSSC is comparable to the natural photosynthetic approach and, herein, the system is able to produce energy by transforming absorbed solar energy into its electrical form. The DSSC device is typically constructed using a dye sensitizer, a metal oxide-based semiconductor, an electrolyte comprising iodide/triiodide ions and a counter electrode [1–3]. The first DSSC patent was submitted in 1977 in the US, in which Prof. Michael Grätzel reported TiO<sub>2</sub> with a polypyridyl complex of ruthenium as an anode. After several efforts, the efficiency of a small area cell has increased from 10% in 1990 to 11.9% in 2012, whereas with large-scale devices, it hardly reaches 5%. Hence, in order to enhance the efficiency, detailed research was carried out on rationally designing the individual components, which include photoanodes, counter electrodes, electrolytes and sensitizers [4,5]. Especially, sensitizers are essential for converting solar energy (photons) into electrical energy (electrons) in DSSC, and thus, numerous metal complexes, organometallics, organic dyes and derivatives were designed and employed as sensitizers. However, ruthenium-based synthetic dyes

have exhibited superior performance as sensitizers, and especially, the DSSCs sensitized using Ru-based N719 have demonstrated the highest efficiency, exceeding 11% [6–8].

The methods used to synthesize organic or metal complex-based dyes involve complex procedures that include multiple steps and expensive chromatographic purification processes [9,10]. Switching from synthetic–organic and inorganic dyes to natural pigments like anthocyanin and chlorophyll, which can be readily derived from plant leaves, fruits, flowers and roots, could certainly address the aforementioned challenges [11,12]. Chlorophyll pigments are typically found in a wide variety of plant components, and each molecule of chlorophyll has four pyrrole rings surrounding a  $Mg^{2+}$  ion, among which one is attached to a phytol tail [13,14]. Chlorophylls are divided into two types, called chlorophyll a and b, that vary in one of the pyrrole rings' at C3 positions in their structures. In chlorophyll b, the formyl (-CHO) chain is attached to the C3 side of the pyrrole ring, but in chlorophyll a, the methyl (-CH<sub>3</sub>) group is attached at the same location [15,16]. The different substituents that make up the chlorophyll a and b pigments result in different light absorbance characteristics [17,18]. Therefore, a broad range of wavelengths that correspond to the visible spectrum's violet, red and blue portions are absorbed by chlorophyll and its derivatives [19,20]. Current state-of-the-art DSSCs are defined by solar-to-electric power conversion efficiencies (PCEs) of 10–13%, with a range of 350–750 nm. The primary barrier to these systems' ability to boost their efficiency further is their lack of absorption in the far-red/near-IR region. The visible radiation (between 350 and 700 nm) makes up about 45% of solar energy that reaches the Earth's surface, whereas red/NIR radiation (between 600 and 1000 nm) makes up around 25%. Thus, the higher current output of the device might be attained by the rational design of materials and molecules for maximum utilization of the solar spectrum [21,22].

Recently, a number of studies have reported that the photovoltaic performance of DSSCs could be rationally tuned by using different natural dyes [23–25]. Wongcharee and his group used natural dyes extracted from blue pea and rosella, as well as a combination of the aforementioned dye extracts, and created three distinct types of DSSCs. The light absorption spectrum of the dye mixture revealed peaks that matched with the distinct natural pigments found in blue pea and rosella. In contrast to the individual component dyes, there was no synergistic photosensitization effect or light absorption from the dye mixture adsorbed on TiO<sub>2</sub> [26]. In a different study, Sengupta and his group extracted dyes from fresh spinach leaves and beetroots and used them to measure photovoltaic performance and achieved 0.29% efficiency with it. This was possible because of the absorbance characteristics of the extracted dyes over a wide range of solar energy [27]. Similarly, Park and his group extracted two separate color dyes (yellow and blue) from Gardenia Jasminoides flowers. The mixture of both dyes shows an increase in the wavelength of light absorption than in specific dyes, which results in higher photovoltaic performance of the device [28]. Despite all these attempts, a lot of efforts are still underway across the globe by different researchers to identify new natural dyes in order to make them competitive in performance with synthetic dyes.

In the quest for natural sources for extracting efficient dyes, Rhodospirillum rubrum (Rh. Sphaeroides) photobacteria (Rh. Sphaeroides) appear to be a very good choice. Rh. Sphaeroides belongs to the Rhodobacteraceae family and is commonly found in both fresh and marine water. Notably, the ability of Rh. Sphaeroides to perform photosynthesis by trapping sunlight has been already well established. It can absorb light and use a mechanism known as anoxygenic photosynthesis to transform the absorbed light into chemical energy because it has pigments called bacteriochlorophylls. Impressed with these characteristics, in this present work, we intended to extract Bacteriopheophytin-a (Bhcl) dye from Rh. Sphaeroides and to synthesize two cationic derivatives, viz. Guanidino-bacteriopheophorbide-a (Gua-Bhcl) and (2-aminoethyl)triphenylphosphono-bacteriopheophorbide-a (2AETPPH-Bhcl), and thereafter to fabricate DSSCs by employing all three compounds as natural sensitizers. The performance of the obtained DSSCs has been probed and correlated with the photophysical and electrochemical properties of the prepared dyes.



Further, the photophysical properties of the extracted dye and its derivatives were investigated by recording their absorbance and emission spectra. The natural dye solution was initially prepared by dissolving 1 mM of dye (2AETPPh-Bhcl, Gua-Bhcl and Bhcl) in deionized water. Both UV-visible absorption and fluorescence emission studies were recorded at room temperature in a 1 cm × 1 cm quartz cuvette. As shown in Figure 3, when dissolved in methanol, at 1 μM concentration, Bhcl exhibits excitation and emission spectra around 775 and 796 nm, respectively. Further, the positively charged Bhcl derivative, Gua-Bhcl exhibits excitation and emission spectra around 756 and 779 nm, and the 2AETPPh-Bhcl exhibits excitation and emission spectra near 754 and 779 nm, respectively. These results infer that the extracted Bhcl and its cationic derivatives exhibit very strong excitation and emission in the NIR region and are thus regarded as potential candidates to be explored as sensitizers in DSSCs. Moreover, the positively charged guanidine and triphenylphosphine group in the derivatives might facilitate firm anchoring of the photosensitizer on the TiO<sub>2</sub> surface to improve the solar energy conversion.

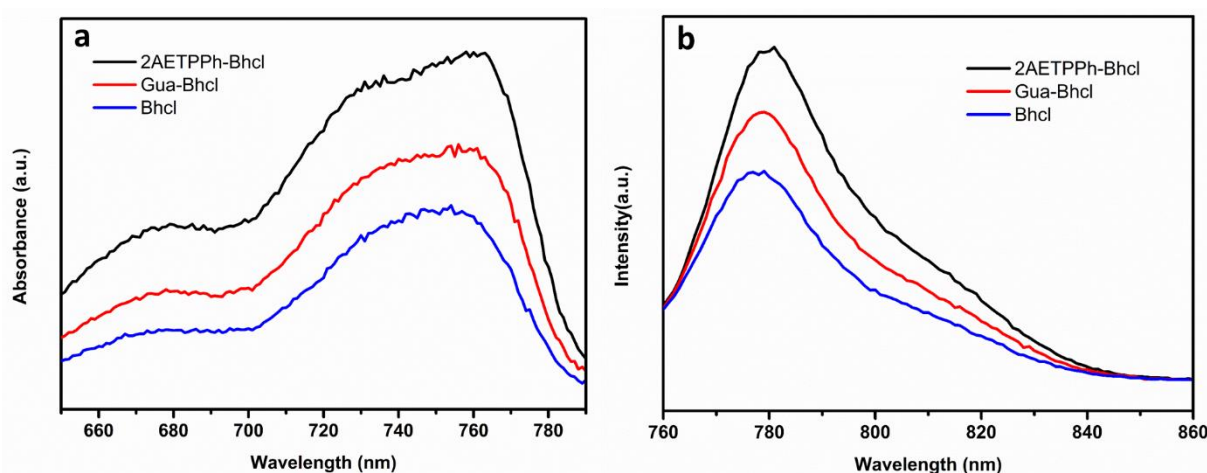


**Figure 3.** (a) Absorbance and (b) emission spectra of Bhcl, Gua-Bhcl and 2AETPPh-Bhcl.

## 2.2. Photovoltaic Performance

The interesting optical performance displayed by Bhcl and its derivatives motivated us to explore their ability as sensitizers in DSSC. Thus, the photovoltaic characteristics of the photoelectrodes fabricated using these new dyes were probed employing a Keithley 4200 source meter. The lamp intensity was kept at 100 mW cm<sup>-2</sup> with an air mass 1.5 filter and the active area of the device was set to 0.25 cm<sup>2</sup>. Figure 4 depicts the typical current–voltage curve of the DSSC sensitized using Bhcl, Gua-Bhcl and 2AETPPh-Bhcl dyes. The photovoltaic parameters obtained for the constructed DSSCs are presented in Table 1, and it can be observed that all three dyes under investigation exhibit reasonable performance as sensitizers towards the construction of DSSCs. The Bhcl dye isolated from the bacteriochlorophyll displayed reasonably good short circuit photocurrent density ( $J_{sc}$ ), open circuit photovoltage ( $V_{oc}$ ), filling factor (FF) and efficiency ( $\eta$ ) values of 0.97 mA cm<sup>-2</sup>, 0.52 V, 0.56 and 0.18%, respectively, obtained with the DSSC sensitized using Bhcl dye. Meanwhile, the derivative Gua-Bhcl exhibited  $J_{sc}$ ,  $V_{oc}$ , FF and  $\eta$  values of 0.99 mA cm<sup>-2</sup>, 0.60 V, 0.60 and 0.25%, respectively, and the derivative 2AETPPh-Bhcl showed  $J_{sc}$ ,  $V_{oc}$ , FF and  $\eta$  values of 1.03 mA cm<sup>-2</sup>, 0.63 V, 0.75 and 0.38%, respectively. Though all the compounds have shown their ability as sensitizers in DSSC, the Gua-Bhcl and 2AETPPh-Bhcl derivatives displayed higher performance than those of Bhcl. This could be because of the cationic charges available on these derivatives, which ensure a uniform dispersion and firm anchoring on the TiO<sub>2</sub> photoanodes. Especially, the 2AETPPh-Bhcl derivative demonstrated excellent photovoltaic parameters compared to the Gua-Bhcl derivative, and this could be attributed to the presence of triphenylphosphine moiety, which can induce steric hindrance and, in turn, could efficiently enhance the open circuit photovoltage through

minimization of the recombination effect. The photovoltaic performance investigations undoubtedly reveal that the isolated Bhcl and the cationic derivatives could be employed as sensitizers for the fabrication of highly efficient DSSCs. The maximum efficiency that could be attained is 0.38% with 2AETPPh-Bhcl derivative as the sensitizer, which is relatively less than many of the synthetic dye-based DSSCs. Even devices fabricated without the presence of any dye have been afforded an efficiency of 0.13% [25]. This efficiency could be significantly improved by the appropriate choice of photoanodes, counter electrodes and semisolid electrolytes, and this work is underway in our laboratory.

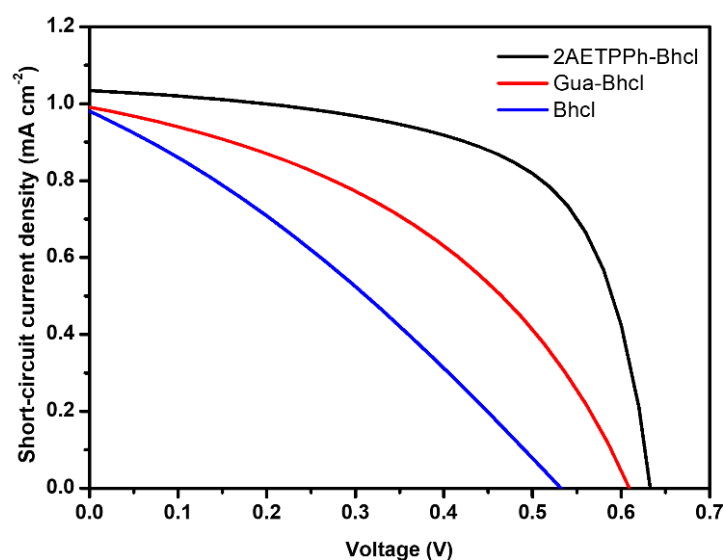


**Figure 4.** J–V curves obtained for DSSCs sensitized with Bhcl, Gua-Bhcl and 2AETPPh-Bhcl.

**Table 1.** Photovoltaic parameters of fabricated DSSCs sensitized using different dyes.

Parameters	Bhcl	Gua-Bhcl	2AETPPh-Bhcl
$V_{oc}$ (V)	0.52	0.60	0.63
$J_{sc}$ ( $\text{mA cm}^{-2}$ )	0.97	0.99	1.03
FF	0.56	0.60	0.75
$\eta$ (%)	0.18	0.25	0.38

The stability of all three dyes was measured by performing current voltage ( $i$ - $V$ ) measurements for 10 days (Figure S4). During the three dyes, 2AETPPh-Bhcl displayed higher stability, which retains 29% of efficiency after 10 days compared to Gua-Bhcl (3.44%) and Bhcl (0.5%). The relatively better stability achieved with 2AETPPh-Bhcl could be due to the uniform and firm anchoring of the dye on the  $\text{TiO}_2$  photoanode.

### 2.3. Atomic Force Microscopic Studies

The coverage of the dye molecules on the surface of the photoanode is a significant factor that decides the final output of the fabricated device. In order to investigate the dispersion of the dyes and their impact on the photovoltaic performance, we envisaged to probe the  $\text{TiO}_2$  photoanodes using atomic force microscopy (AFM). To develop  $\text{TiO}_2$ -coated films,  $\text{TiO}_2$  was deposited on an FTO plate and calcined at 500 °C, after which the obtained film was immersed in the respective dye. Thereafter, the film was dried and then washed with water and ethanol and subjected to AFM measurements. The topography images of  $\text{TiO}_2$  sensitized with Bhcl, Gua-Bhcl and 2AETPPh-Bhcl dyes were recorded and presented in Figure 5. As depicted in Figure 5, a higher degree of inhomogeneity can be observed in the photoanode surface, which is sensitized with the Bhcl dye (Figure 5a). A relatively better surface coverage could be observed in the photoanode surface sensitized with Gua-Bhcl (Figure 5b). Notably, an ample surface coverage indicative of a uniform

dispersion can be seen in the 2AETPPh-Bhcl dye-sensitized TiO<sub>2</sub> photoanode (Figure 5c). The relatively better surface coverage observed with Gua-Bhcl and 2AETPPh-Bhcl dyes is again ascribed to the electrostatic interaction between the positive charge on these dyes and the photoanodes. The surface roughness factor of the dye-loaded TiO<sub>2</sub> photoanode was calculated to be 78 nm, 95 nm and 115 nm for Bhcl, Gua-Bhcl and 2AETPPh-Bhcl, respectively. Thus, it can be concluded that the higher degree of coverage in the 2AETPPh-Bhcl dye-sensitized TiO<sub>2</sub> has led to the enhanced performance of the constructed DSSC device than that observed with Bhcl and Gua-Bhcl. These results are well in agreement with the photovoltaic parameters recorded using J–V curves.

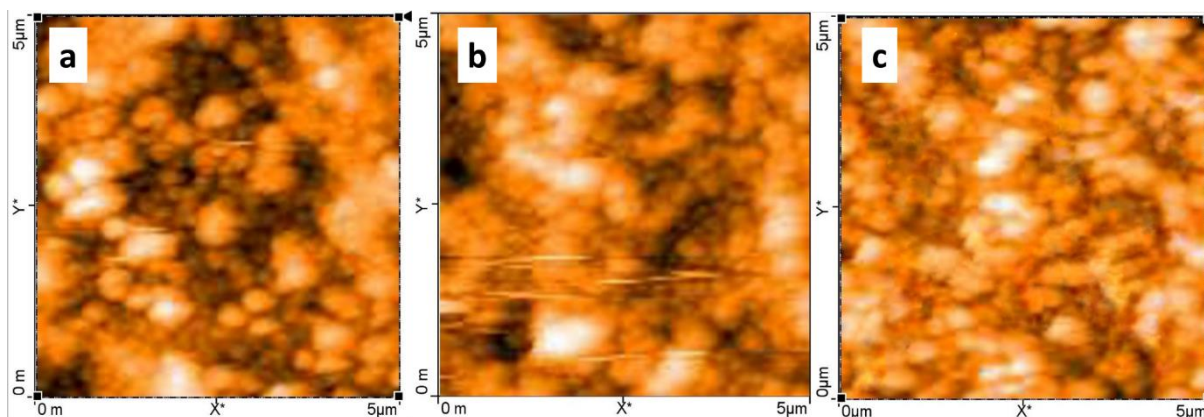


**Figure 5.** AFM images of TiO<sub>2</sub> photoanodes sensitized using (a) Bhcl, (b) Gua-Bhcl and (c) 2AETPPh-Bhcl dyes.

The photoconversion efficiency of the DSSC is dependent on several factors, which include the wettability of the dye, charge polarization of the dye and also the amount of dye loading on the photoanode. Higher loading of the dye on the photoanode can establish a greater number of electron injections into the conduction band of the TiO<sub>2</sub>, thereby delivering more carrier diffusion across the device [26]. As observed from our AFM images, the AETPPh-Bhcl dye displayed excellent and uniform loading on the TiO<sub>2</sub> surface. The roughness factor of the dye-loaded TiO<sub>2</sub> is also a key factor that decides the rate of photoconversion since the surface texture of the photoanode can influence the photon-reflecting angle and it can make the photon bounce back and deliver higher current generation indirectly. Here, the higher roughness factor (115 nm) of AETPPh-Bhcl-sensitized TiO<sub>2</sub> delivers maximum photocurrent compared to the other two counterparts.

#### 2.4. Electrochemical Investigations

In order to understand the performances of the Bhcl dye and its derivatives as sensitizers in DSSC, their electrochemical properties, such as redox behavior, and their conductivity were investigated by performing cyclic voltammetry (CV) and electrochemical impedance spectroscopy (EIS). The CV analysis of all three dyes was carried out employing nickel foam as the working electrode, Pt as the counter electrode, Ag/AgCl as the reference electrode and 2 M KOH as the electrolyte using a three-electrode setup with a PGSTAT204 Autolab workstation (Metrohm, The Netherlands). As observed from Figure 6a, all three dyes exhibit well-defined oxidation/reduction peaks indicative of their excellent redox behavior, and because of this, all dyes have shown reasonable photovoltaic performances. However, upon comparison, the Gua-Bhcl and 2AETPPh-Bhcl dyes display a better voltammetric response with higher current density when compared to that of Bhcl. The presence of cationic substituents in the Gua-Bhcl and 2AETPPh-Bhcl might have facilitated electron shuttling, which resulted in higher current densities. This, in turn, is reflected in the higher photovoltaic performance of Gua-Bhcl and 2AETPPh-Bhcl than that observed with Bhcl.

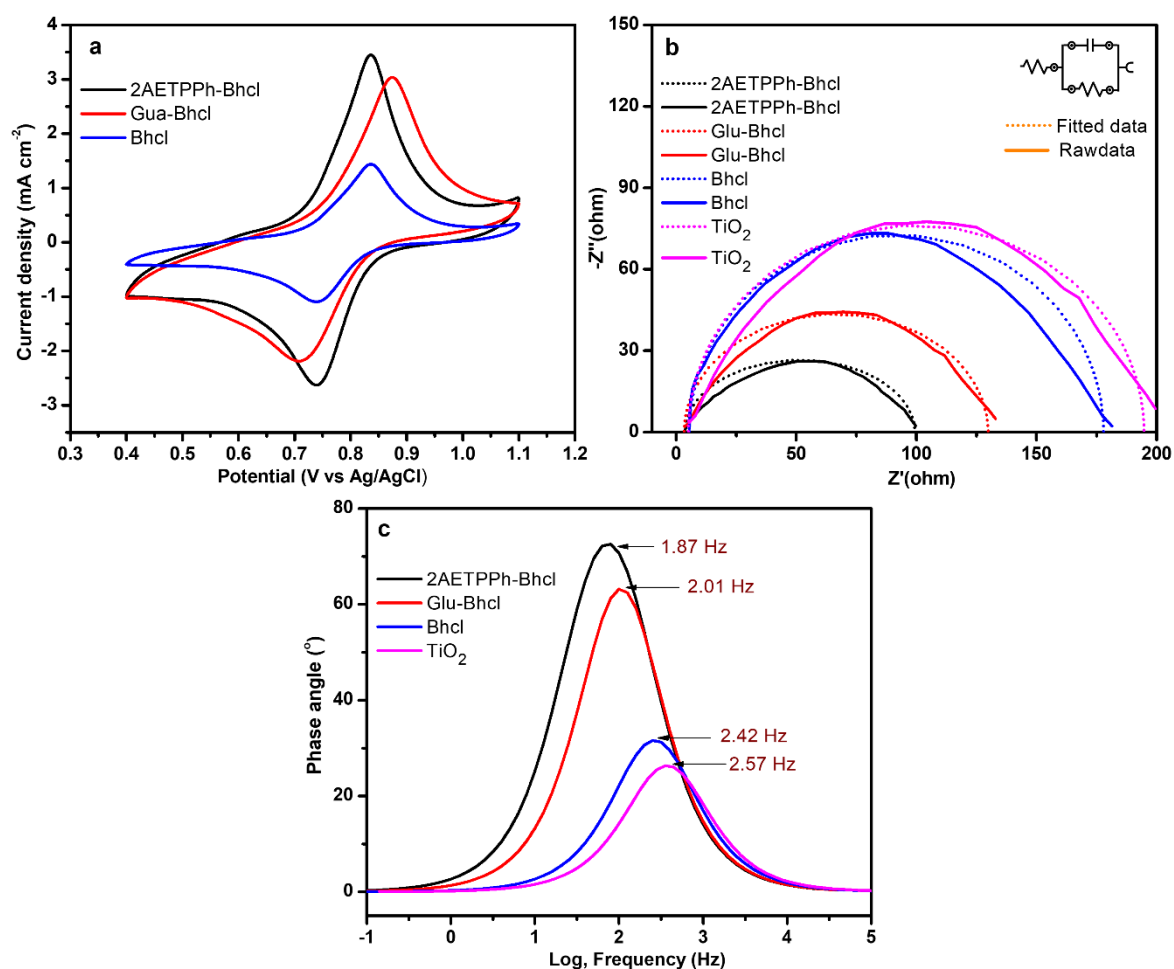


**Figure 6.** (a) Cyclic voltammograms of Ni foam with Bhcl, Gua-Bhcl and 2AETPPh-Bhcl (electrolyte: 2 M KOH). (b) Electrochemical impedance spectra and (c) Bode plots of DSSCs sensitized with Bhcl, Gua-Bhcl and 2AETPPh-Bhcl dyes.

EIS was employed mainly to probe the interfacial kinetics and charge transport properties of the fabricated DSSCs. The EIS plot of DSSC contains three main regions, in which the higher frequency region denotes the resistance between the FTO and  $\text{TiO}_2$  interface [29,30]. The lower frequency region denotes the charge transfer resistance between the counter electrode and electrolyte interface and the middle portion denotes the recombination resistance between the dye and electrolyte. A smaller semicircle represents the low recombination as well as higher charge kinetics, and this would facilitate the performance of DSSC [31,32]. The EIS spectra of the unmodified  $\text{TiO}_2$  and the dye-coated  $\text{TiO}_2$  have been recorded (Figure 6b). It could be observed that the unmodified  $\text{TiO}_2$  exhibits a very high  $R_{ct}$  value of  $190 \Omega$ , which could be due to the high repulsion between the  $\text{TiO}_2$  photoanode and the negatively charged iodide ions in the electrolyte. Upon coating with Bhcl, the  $R_{ct}$  value ( $173 \Omega$ ) did not change significantly. However, upon coating with Gua-Bhcl and 2AETPPh-Bhcl, the  $R_{ct}$  value reduced drastically to  $126 \Omega$  and  $96 \Omega$ , respectively. Since the positively charged dyes Gua-Bhcl and 2AETPPh-Bhcl anchor on the  $\text{TiO}_2$  photoanodes, the repulsion between the electrolyte and photoanode might have significantly reduced, thus resulting in a reduced  $R_{ct}$  value. Likewise, the solution resistance ( $R_s$ ) values of 2AETPPh-Bhcl, Gua-Bhcl, Bhcl and unmodified  $\text{TiO}_2$ -based devices were found to be  $3.21$ ,  $3.56$ ,  $5.5$  and  $5.05 \Omega$ , respectively. The low  $R_s$  and  $R_{ct}$  value of a 2AETPPh-Bhcl-based device denotes the low recombination and high conductivity, which lead to enhanced photovoltaic performance.

From the Bode plot, it can be seen that the Gua-Bhcl and 2AETPPh-Bhcl dye-sensitized DSSC devices showcase a lower frequency shift along with a greater phase angle, which

depicts the longer electron lifetime of the constructed device compared to the Bhcl and bare TiO<sub>2</sub>-based DSSC [33,34]. The electron lifetime obtained using the equation  $\tau_e = (2\pi f_{\max})^{-1}$  for TiO<sub>2</sub>, Bhcl, Gua-Bhcl and 2AETPPh-Bhcl dyes were found to be 61.95 ms, 66.20 ms, 79.17 ms and 85.05 ms, respectively. The maximum electron lifetime observed with 2AETPPh-Bhcl dye-based DSSC (compared to Bhcl and Gua-Bhcl) suggests the lower recombination rates due to the bulkier triphenylphosphine moiety, thereby enhancing the electron density and photovoltaic performance of the fabricated DSSC.

Overall, the photovoltaic performance of DSSCs sensitized with Bhcl, Gua-Bhcl and 2AETPPh-Bhcl are comparable to or better than many of the recently reported natural dyes, and the performances are compared in Figure 7.

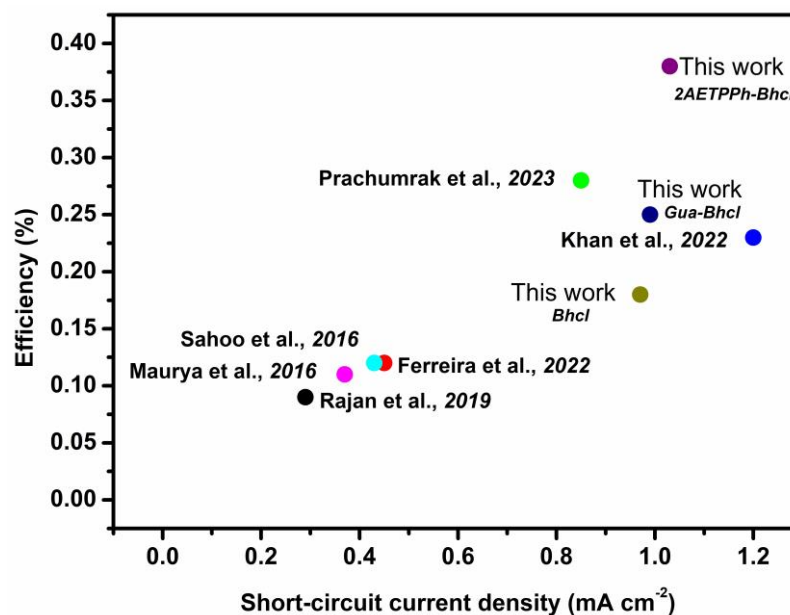


Figure 7. Comparative photovoltaic performance of DSSCs sensitized using natural dyes [35–40].

### 3. Materials and Methods

#### 3.1. Chemicals

2-(1H-7-Azabenzotriazol-1-yl)-1,1,3,3-tetramethyl uronium hexafluorophosphate methanaminium (HATU) was obtained from Genscript Inc. (Piscataway, NJ, USA). Guanidine hydrochloride, (2-aminoethyl) triphenylphosphonium bromide, diisopropylethylamine (DIPEA), dimethyl sulfoxide (DMSO) and all other reagents were purchased from Sigma-Aldrich.

#### 3.2. Characterization

The extracted dye and their derivatives were characterized using triple quadrupole mass spectrometer (Shimadzu LCMS-8060: Kyoto, Japan). Agilent Cary 60 UV-Vis spectrophotometer was used to record the absorption spectra of the dye. For the emission spectra, Agilent Cary Eclipse Fluorescence Spectrophotometer with an inbuilt pulsed diode LASER was used for excitation. Atomic force microscopy (AFM-Park XE7, in 1  $\mu\text{m} \times 1 \mu\text{m}$  scan area, Yongin City, South Korea) was used to analyze the dye loading and uniformity of the photoanode surface. Compounds were purified by preparative reverse phase (RP)-HPLC (Waters, xTerra C18 10  $\mu\text{m}$ ; 19 mm  $\times$  250 mm, Granada, Spain) and analyzed using UPLC (Acquity, BEH C18, 1.7  $\mu\text{m}$ , 2.1 mm  $\times$  50 mm). Purity of the isolated compounds was analyzed by analytical HPLC using either achiral column (XSelect CHC PFP C18, 2.5  $\mu\text{m}$ , 4.6 mm  $\times$  150 mm, USA) and chiral column [Chiralpak ZWIX(+) 3  $\mu\text{m}$ , 3.0 mm  $\times$  150 mm] with solvent gradient of 3% B to 30% B in 30 min with run time of 45 min (where A = 30 mM ammonium acetate and B = acetonitrile) unless otherwise noted.

All the isolated compounds demonstrated  $\geq 95\%$  purity at  $\lambda = 270$  and/or  $770$  nm in the aforementioned analytical HPLC method.

### 3.3. Isolation of Bacteriopheophytine-a (Bhcl) from *Rh. Sphaeroides*

In the typical extraction process, *Rh. Sphaeroides* was added to 1-propanol with continuous  $N_2$  flow under stirring condition for 12 h at room temperature. The obtained mixture was filtered under vacuum using Whatman no. 1 filter paper, and then the residue was washed several times with 1-propanol until the solution became colorless. The obtained extract was labeled as bacteriochlorophyll-a and the product was confirmed by LCMS analysis with a molecular weight of 911.1 ( $M + 1$ ). In order to obtain bacteriopheophytine-a (Bhcl), 20 mL of con. HCl was added to the colorless solution and stirred for another 20 min (Figure 1). Afterwards, the solution was transferred to 5% NaCl (1.5 L) and purified with  $CH_2Cl_2$  using silica column, to obtain the Bhcl product. The obtained Bhcl was confirmed by LCMS analysis (Figure S1) and the isolated product was obtained with a molecular weight of 611.3 ( $M + 1$ ).

### 3.4. Synthesis of Cationic Derivatives of Bhcl

For the synthesis of the cationic derivatives, Bhcl, diisopropylethylamine and HATU were taken in 1:5:1 proportion in dimethyl sulfoxide and the mixture was subjected to stirring under Ar flow for 30 min. To synthesize Guanidino-bacteriopheophorbide-a, thrice the amount of guanidine hydrochloride salt was added to the reaction mixture and the stirring continued at RT overnight. Similarly, in order to obtain (2-aminoethyl)triphenylphosphonobacteriopheophorbide-a, thrice the amount of (2-aminoethyl)triphenylphosphonium bromide was added to the reaction mixture and the stirring continued overnight at room temperature. Thereafter, the obtained products were subjected to purification using preparative reverse-phase HPLC comprising a mobile phase of A = 20 mM ammonium acetate buffer at pH 7 and B = acetonitrile; gradient 0–50% B in 30 min,  $13 \text{ mLmin}^{-1}$ ,  $\lambda = 280$  nm. Finally, the purified fractions were analyzed using LCMS (Figures S2 and S3), then pooled and lyophilized to furnish Gua-Bhcl [653.7 ( $M + 1$ )] and 2AETPh-Bhcl [899.06 ( $M - H_2O$ )].

### 3.5. Electrochemical Techniques

The electrochemical investigations including cyclic voltammetry (CV) and electrochemical impedance spectroscopy (EIS) were performed with three-electrode setup with PGSTAT204 Autolab workstation (Metrohm, The Netherlands). CV was carried out employing nickel foam as working electrode, Pt as counter, Ag/AgCl as reference electrodes and 2 M KOH as the electrolyte. The frequency range for the EIS was set as  $10^{-2}$  to  $10^5$  Hz. A bias voltage of 0 V is applied in dark condition to the fabricated DSSC devices.

### 3.6. Device Fabrication

Initially, glass substrates covered with fluorine-doped tin oxide (FTO) (surface resistivity =  $7.5 \Omega \text{ cm}^{-2}$ ) were cleaned by sonication in acetone and ethanol for around 15 min each. To make a semisolid  $TiO_2$  slurry, 100 mg of P25- $TiO_2$  was ground using an agate mortar and pestle with a few drops of water, acetylacetone and Triton X-100. To construct  $TiO_2$ -coated thin films,  $TiO_2$  slurry was coated over FTO plate using doctor blading method followed by calcination for 30 min at  $500^\circ\text{C}$ . Further, the constructed  $TiO_2$  thin films were immersed separately in the respective extracted natural dye. The dye-coated thin films were then dried and washed with water and ethanol. The photoanode was coated with the respective dye (with thickness of  $12 \mu\text{m}$ ) and the counter electrode on another FTO substrate was coated with platinum (Pt) (with thickness of 5 nm). The counter electrode was prepared as follows: 0.01 M of  $H_2PtCl_6$  was dissolved in isopropanol and the obtained homogeneous solution was drop-casted on a precleaned FTO, which was annealed at  $450^\circ\text{C}$  for 30 min to obtain Pt CE. Subsequently, the DSSC device was generated upon injection of a minute quantity of  $I^-/I_3^-$  electrolyte in between the photocathode and the dye-coated photoanode.

#### 4. Conclusions

In summary, the Bacteriopheophytine-a (Bhcl) dye was extracted from *Rh. Sphaeroides* photobacteria and two of its derivatives, viz. Gua-Bhcl and 2AETPPh-Bhcl, which were synthesized and employed as natural sensitizers for the construction of efficient DSSCs. The photophysical investigation of Bhcl and the cationic derivatives Gua-Bhcl and 2AETPPh-Bhcl showed excellent absorbance around the NIR region. The photovoltaic performance of all three dyes was probed, among which the DSSCs sensitized with the cationic derivatives Gua-Bhcl and 2AETPPh-Bhcl exhibited better performance, which could be due to the uniform dispersion of the cationic dyes on the TiO<sub>2</sub> photoanodes through electrostatic interaction. Especially, the 2AETPPh-Bhcl demonstrated superior photovoltaic performance with an efficiency of 0.38% at  $J_{SC}$  of 1.03 mA cm<sup>-2</sup>, and this performance is comparable to or better than many of the naturally obtained dyes. The topological investigations using AFM and electrochemical studies using CV and EIS also evidence the superior performance obtained with 2AETPPh-Bhcl dye as the sensitizer. This investigation paves the way for the extraction of more natural dyes and designing task-specific derivatives for the construction of DSSCs and other optical devices.

**Supplementary Materials:** The following information is given in the supporting information at: <https://www.mdpi.com/article/10.3390/molecules29050931/s1>. Figure S1: LCMS of Bhcl; Figure S2: LCMS of Gua-Bhcl; Figure S3: LCMS of 2AETPPh-Bhcl; Figure S4. Stability of the DSSCs sensitized with different dyes. Table S1: Comparative photovoltaic performance of DSSCs sensitized using natural dyes.

**Author Contributions:** Conceptualization, R.S.K. and A.I.A.; Methodology, A.I.A., K.I.A.-S. and N.A.; Validation, R.S.K.; Formal analysis, A.I.A. and N.A.; Investigation, R.S.K., N.A. and A.I.A.; Resources, R.S.K.; Writing—original draft, A.I.A., R.S.K. and N.A.; Writing—review and editing, R.S.K. and N.A.; Visualization, A.I.A. and K.I.A.-S.; Supervision, A.I.A. and R.S.K.; Funding acquisition, R.S.K. and A.I.A. All authors have read and agreed to the published version of the manuscript.

**Funding:** The authors extend their appreciation to the Deputyship for Research and Innovation, “Ministry of Education” in Saudi Arabia for funding this research work through the project number IFKSUDR\_E114.

**Institutional Review Board Statement:** Not applicable.

**Informed Consent Statement:** Not applicable.

**Data Availability Statement:** Data are contained within the article and Supplementary Materials.

**Conflicts of Interest:** The authors declare no conflict of interest.

#### References

1. Zhou, H.; Wu, L.; Gao, Y.; Ma, T. Dye-sensitized solar cells using 20 natural dyes as sensitizers. *J. Photochem. Photobiol. A* **2018**, *219*, 188–194. [CrossRef]
2. Geetam, R.; Anil, K.; Perapong, T.; Bhupendra, G. Natural dyes for dye sensitized solar cell: A review. *Renew. Sustain. Energy Rev.* **2017**, *69*, 705–718.
3. Napitupulu, N.D.; Rahman, N. Plant Leaf Chlorophyll Based DSSC Solar Cell with ITO Transparent nanoparticle Alloy. *Int. J. Heat Technol.* **2023**, *41*, 462–468.
4. Parisi, M.L.; Maranghi, S.; Basosi, R. The evolution of the dye sensitized solar cells from Grätzel prototype to up-scaled solar applications: A life cycle assessment approach. *Renew. Sustain. Energy Rev.* **2014**, *39*, 124–138. [CrossRef]
5. Takagi, K.; Magaino, S.; Saito, H.; Aoki, T.; Aoki, D. Measurements and evaluation of dye-sensitized solar cell performance. *J. Photochem. Photobiol. C* **2013**, *14*, 1–12. [CrossRef]
6. Kakiage, K.; Aoyama, Y.; Yano, T.; Oya, K.; Fujisawa, J.; Hanaya, M. Highly-efficient dye-sensitized solar cells with collaborative sensitization by silyl-anchor and carboxy-anchor dyes. *Chem. Commun.* **2015**, *51*, 15894–15897. [CrossRef]
7. Leonardo, R.B.; Higor, O.; Arcano, M.B.; Rajendran, S.B.; Sebastian, R.; Caue, R.; Ana, L.F. Evaluation of Solar Conversion Efficiency in Dye-sensitized Solar Cells Using Natural Dyes Extracted from *Alpinia purpurata* and *Alstroemeria* Flower Petals as Novel Photosensitizers. *Colorants* **2023**, *2*, 618–631.
8. Robledo, A.G.F.; Enríquez, J.P.; Avendaño, C.A.M. Characterization of natural dyes on ZnO and TiO<sub>2</sub> thin films for applications in DSSC. *J. Mater. Sci. Mater. Electron.* **2023**, *34*, 980. [CrossRef]

9. Nasim, S.; Monas, S.; Rabia, G.; Khalid, J.; Mahroze, M.; Aneel, P.; Abdul, G. Fabrication of DSSC based on Capsicum annum and Tamarindus indica plant seeds extract as natural photosensitizers. *Solar Energy* **2023**, *257*, 314–323.
10. Rajaramanan, T.; Heidari Gourji, F.; Elilan, Y. Natural sensitizer extracted from Mussaenda erythrophylla for dye-sensitized solar cell. *Sci. Rep.* **2023**, *13*, 13844. [[CrossRef](#)]
11. Tadesse, S.; Abebe, A.; Chebude, Y.; Garcia, I.V.; Yohannes, T. Natural dye-sensitized solar cells using pigments extracted from Syzygium guineense. *J. Photonics Energy* **2012**, *2*, 027001. [[CrossRef](#)]
12. Sabra, Y.; Talal, K.; Najla, A.; Khurshid, A. Porphyrin-Anhydride Co-Sensitization Strategy for Enhanced Photovoltaic Performance in DSSC: A Combined Experimental and Theoretical Approach. *Polyhedron* **2023**, *246*, 116675.
13. Arof, A.K.; Ping, T.L. Chlorophyll as photosensitizer in dye-sensitized solar cells. *Chlorophyll* **2017**, *7*, 105–121.
14. Conrad, F.; Wilke, D.; Caroline, M.B.; Johannes, S.; Franz, P.M. Synthesis of Donor Substituted Chlorophyll Derivatives for Application in Dye Sensitized Solar Cells. *EurJOC* **2023**, *26*, 202300816.
15. Kannangara, C.G. Biochemistry and molecular biology of chlorophyll synthesis. *Photosynth. Appar.* **2012**, *7*, 301.
16. Kavin, P.; Wasan, M.; Bhalang, S.; Samuk, P.; Vittaya, A. Dye-sensitized solar cells based on purple corn sensitizers. *Appl. Surf. Sci.* **2016**, *380*, 101–107.
17. Yuxiao, C.; Wenjie, Z.; Shin, O.; Xiao, F.W.; Hitoshi, T. Fabrication and performance of all-solid-state dye-sensitized solar cells using synthetic carboxylated and pyridylated chlorophyll derivatives. *J. Photochem. Photobiol. A* **2018**, *353*, 625–630.
18. Aung, S.H.; Yan, H.; Than, Z.O.; Gerrit, B. Kinetic study of carminic acid and santalin natural dyes in dye-sensitized solar cells. *J. Photochem. Photoiol. A Chem.* **2016**, *325*, 1–8. [[CrossRef](#)]
19. Li, Y.; Wang, J.; Yan, C.; Zhang, S.; Cui, N.; Liu, Y.; Li, G.; Cheng, P. Optical and electrical losses in semitransparent organic photovoltaics. *Joule* **2024**. [[CrossRef](#)]
20. Wang, J.; Xue, P.; Jiang, Y.; Huo, Y.; Zhan, X. The principles, design and applications of fused-ring electron acceptors. *Nat. Rev. Chem.* **2022**, *6*, 614–634. [[CrossRef](#)]
21. Syafnar, R.; Gomesh, N.; Irwanto, M.; Fareq, M.; Irwan, Y.M. Chlorophyll pigments as nature-based dye for dye-sensitized solar cell (DSSC). *Energy Procedia* **2015**, *79*, 896–902. [[CrossRef](#)]
22. Hughes, N.M.; Smith, W.K. Attenuation of incident light in *Galax urceolata* (Diapensiaceae): Concerted influence of adaxial and abaxial anthocyanic layers on photoprotection. *Am. J. Bot.* **2007**, *94*, 784–790. [[CrossRef](#)] [[PubMed](#)]
23. Prabavathy, N.; Shalini, S.; Balasundaraprabhu, R.; Dhayalan, V.; Prasanna, S.; Pravin, W.; Muthukumarasamy, N. Effect of solvents in the extraction and stability of anthocyanin from the petals of *Caesalpinia pulcherrima* for natural dye sensitized solar cell applications. *J. Mater. Sci. Mater. Electron.* **2017**, *28*, 9882–9892. [[CrossRef](#)]
24. Yuly, K.; Aulia, S.H.; Diana, V.W.; Riki, S. Natural resources for dye-sensitized solar cells. *Heliyon* **2021**, *7*, e08436.
25. Dao, V.D.; Larina, L.L.; Choi, H.S. Plasma Reduction of Nanostructured TiO<sub>2</sub> Electrode to Improve Photovoltaic Efficiency of Dye-Sensitized Solar Cells. *J. Electrochem. Soc.* **2014**, *161*, 896–902. [[CrossRef](#)]
26. Dao, V.D. Comment on “Energy storage via polyvinylidene fluoride dielectric on the counter electrode of dye-sensitized solar cells” by Jiang et al. *J. Power Sources* **2017**, *337*, 125–129. [[CrossRef](#)]
27. Akula, S.T.; Abhishek, S.; Jena, A.K.S.; Manish, K.T.; Archana, K.; Subhash, C.Y.; Parasharam, M.S. Optimal processing methodology for futuristic natural dye-sensitized solar cells and novel applications. *Dyes Pigm.* **2023**, *210*, 110997.
28. Wongcharee, K.; Meeyoo, V.; Chavadej, S. Dye-sensitized solar cell using natural dyes extracted from rosella and blue pea flowers. *Sol. Energy Mater. Sol. Cells* **2007**, *91*, 566–571. [[CrossRef](#)]
29. Sengupta, D.; Mondal, B.; Mukherjee, K. Visible light absorption and photo-sensitizing properties of spinach leaves and beetroot extracted natural dyes. *Spectrochim. Acta A Mol. Biomol. Spectrosc.* **2015**, *148*, 85–92. [[CrossRef](#)]
30. Park, K.H.; Tae, Y.K.; Ju, Y.P.; Jin, E.M.; Yim, S.H.; John, G.F.; Jae, W.L. Photochemical properties of dye-sensitized solar cell using mixed natural dyes extracted from Gardenia Jasminoide Ellis. *J. Electroanal. Chem.* **2013**, *689*, 21–25. [[CrossRef](#)]
31. Soosairaj, A.; Pabba, D.P.; Gunasekaran, A. Synergetic impact of natural light harvesting materials to reduce the recombination rate and improve the device performance of dye sensitized solar cells. *J. Mater. Sci. Mater. Electron.* **2023**, *34*, 1748. [[CrossRef](#)]
32. Orona, N.A.; Aguilar, H.I.; Nigam, K.D.P.; Cerdan, P.A.; Ornelas, S.N. Alternative Sources of Natural Photosensitizers: Role of Algae in Dye-Sensitized Solar Cell. *J. Biotechnol.* **2021**, *332*, 29–53. [[CrossRef](#)]
33. Zubaidah, S.; Chin, W.L.; Joon, C.J. An investigation of the dye-sensitized solar cell performance using graphene-titania (TrGO) photoanode with conventional dye and natural green chlorophyll dye. *Mater. Sci. Semicond. Process.* **2018**, *74*, 267–276.
34. Sinha, D.; De, D.; Ayaz, A. Photo sensitizing and electrochemical performance analysis of mixed natural dye and nanostructured ZnO based DSSC. *Sadhana* **2020**, *45*, 175. [[CrossRef](#)]
35. Maurya, I.C.; Gupta, A.K.; Srivastava, P.; Bahadur, L. Natural dye extracted from Saraca asoca flowers as sensitizer for TiO<sub>2</sub>-based dye-sensitized solar cell. *J. Sol. Energy Eng.* **2016**, *138*, 051006. [[CrossRef](#)]
36. Ferreira, B.C.; Suresh, B.; Conceicao, L.; Cunha, H.O.; Sampaio, D.M.; Samyn, L.M.; Barros, A.L.F. Performance evaluation of DSSCs using naturally extracted dyes from petals of *Lantana repens* and *Solidago canadensis* flowers as light-harvesting units. *Ionic* **2022**, *28*, 5233–5242. [[CrossRef](#)]
37. Prachumrak, N.; Prajudtasri, N.; Kitisriworaphan, W. Novel photosensitizer from red lotus flower extract for natural dye-sensitized solar cells. *Suranaree J. Sci. Technol.* **2023**, *30*, 1–8. [[CrossRef](#)]

38. Khan, A.A.; Syarifah, A.M.Y.; Mamat, M.H.; Yahaya, S.Z.; Setumin, S.; Ibrahim, M.N.; Daud, K.; Abdullah, M.H. Magnesium sulfate as a potential dye additive for chlorophyll-based organic sensitiser of the dye-sensitised solar cell (DSSC). *Spectrochim. Acta A* **2022**, *274*, 121140. [[CrossRef](#)] [[PubMed](#)]
39. Sahoo, S.S.; Salunke-Gawali, S.; Kadam, V.S.; Pathan, H.M. Canna lily red and yellow flower extracts: A new power source to produce photovoltage through dye-sensitized solar cells. *Energy Fuels* **2020**, *34*, 9674–9682. [[CrossRef](#)]
40. Rajan, A.K.; Cindrella, L. Studies on new natural dye sensitizers from *Indigofera tinctoria* in dye-sensitized solar cells. *Opt. Mater.* **2019**, *88*, 39–47. [[CrossRef](#)]

**Disclaimer/Publisher’s Note:** The statements, opinions and data contained in all publications are solely those of the individual author(s) and contributor(s) and not of MDPI and/or the editor(s). MDPI and/or the editor(s) disclaim responsibility for any injury to people or property resulting from any ideas, methods, instructions or products referred to in the content.